

# Strongly Correlated Electrons in the $[\text{Ni}(\text{hmp})(\text{ROH})\text{X}]_4$ Single Molecule Magnet: A DFT+U Study

Chao Cao,<sup>1,2</sup> Stephen Hill,<sup>1</sup> and Hai-Ping Cheng<sup>1,2</sup>

<sup>1</sup>Department of Physics, University of Florida, Gainesville, FL 32611, U.S.A.

<sup>2</sup>Quantum Theory Project, University of Florida, Gainesville, FL 32611, U.S.A.

(Dated: October 31, 2018)

The single-molecule magnet  $[\text{Ni}(\text{hmp})(\text{MeOH})\text{Cl}]_4$  is studied using both density functional theory (DFT) and the DFT+U method, and the results are compared. By incorporating a Hubbard-U like term for both the nickel and oxygen atoms, the experimentally determined ground state is successfully obtained, and the exchange coupling constants derived from the DFT+U calculation agree with experiment very well. The results show that the nickel 3d and oxygen 2p electrons in this molecule are strongly correlated, and thus the inclusion of on-site Coulomb energies is crucial to obtaining the correct results.

PACS numbers: 75.50.Xx, 75.30.Gw, 71.15.Mb, 71.10.Fd, 73.20.At

Single-molecule magnets (SMMs) have drawn much attention since their discovery in 1991 [1, 2, 3]. SMM crystals contain ordered arrays of molecular nanomagnets, each possessing a large spin ground state ( $S = 10$  for  $\text{Mn}_{12}\text{-Ac}$ ) and a significant uniaxial magneto-anisotropy ( $DS_z^2$ , with  $D < 0$ ). These two ingredients give rise to a magnetic spectrum for an isolated molecule in which the lowest lying levels correspond to the ‘spin-up’ and ‘spin-down’ states ( $m_s = \pm S$ ), separated by an energy barrier of order  $DS^2$ . This barrier results in magnetic bistability and hysteresis at low temperatures ( $k_B T \ll DS^2$ ). In contrast to bulk ferromagnets, however, this hysteresis is intrinsic to the individual molecules. There has, therefore, been much interest in the potential implementation of SMMs as the elementary memory units in both classical and quantum computers.

For most transition metal complexes (including  $\text{Mn}_{12}\text{-Ac}$ ), the intramolecular superexchange between the constituent ions is predominantly antiferromagnetic (AFM). Nevertheless, due to spin frustration effects, uncompensated moments of many tens of  $\mu_B$  are often realized. However, the ability to engineer pure ferromagnetic superexchange within a molecule is highly desirable [4], because this ultimately removes one of the many challenges in designing new and better SMMs. A relatively new series which has attracted recent interest is  $[\text{Ni}(\text{hmp})(\text{ROH})\text{Cl}]_4$  [5, 6, 7, 8, 9] (hereon denoted  $\text{Ni}_4$ ), where hmp is the anion of 2-hydroxymethylpyridine, and R is an alkyl substituent such as methyl, ethyl, etc. Several experiments, including EPR studies [6] and magnetic susceptibility measurements [5] clearly show that the ground state of  $\text{Ni}_4$  is ferromagnetic with total spin  $S = 4$ . In this letter, we present the results of detailed density functional theory (DFT) calculations (including on-site Coulomb energies) which provide crucial insights into the origin of this ferromagnetic state.

While DFT [10] has successfully explained the properties of a variety of SMMs, including  $\text{Mn}_{12}$ ,  $\text{Mn}_4$ ,  $\text{Co}_4$ ,  $\text{Fe}_4$  [11, 12, 13, 14, 15], and even some other nickel based SMMs [16], it has so far failed miserably for  $\text{Ni}_4$ . Not only were the early theoretical attempts unable to reproduce the correct ground state, but the resulting coupling constants were also found to be antiferromagnetic, and orders of magnitude higher

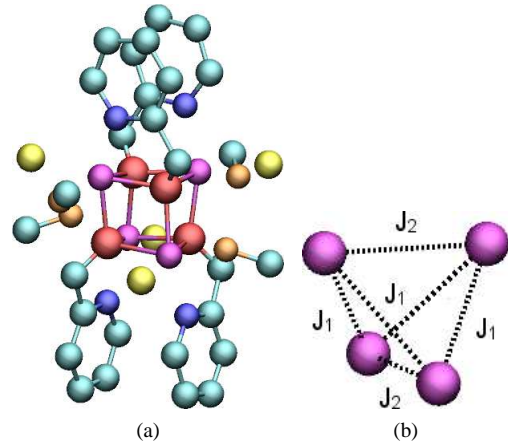


FIG. 1: Optimized structure (a) and exchange-coupling scheme (b) of  $[\text{Ni}(\text{hmp})(\text{MeOH})\text{Cl}]_4$ . Magenta atoms are Ni; red atoms O(1); yellow atoms Cl; orange atoms other oxygens (i.e. O(2)); blue atoms N; and gray atoms C. The Ni and O(1) atoms form a slightly distorted cube.

than the experimental values [17]. It was also found in the calculation that the spin density is not quite localized around the nickel atoms, as expected. Thus, it has been suggested that the discrepancy between theory and experiments might arise due to the small ‘‘spin density leakage’’ in this system, resulting in spin delocalization.

There is another possibility. Due to the localized nature of 3d electrons, transition metal dioxides, including nickel oxides, are known to be strongly correlated materials. The functioning core of  $[\text{Ni}(\text{hmp})(\text{ROH})\text{Cl}]_4$ , on the other hand, is a cubic tetra-nickel oxide ( $\text{Ni}_4\text{O}_4$ ), which is structurally very close to the nickel oxide complex. Therefore, it is more probable that the lack of strong correlation in DFT is responsible for this failure, and the ‘‘spin density leakage’’ is just an artifact. To justify this speculation, we calculated the electronic structure of  $[\text{Ni}(\text{hmp})(\text{MeOH})\text{Cl}]_4$  using both the DFT and DFT+U methods. The latter was introduced by V. I. Anisimov et al. [18] and simplified by M. Cococcioni et al. [19].

All the reported calculations were done using the PWSCF

package [20], which utilizes PBE exchange-correlation functionals [21], ultrasoft pseudopotentials [22], and a plane-wave basis-set. We respectively chose energy cut-offs for the wave functions and charge densities to be 40 Ry and 400 Ry to ensure total energy convergence. The structure of the molecule was optimized with a fixed total spin  $S = 4$  until the force on each atom was smaller than  $0.01 \text{ eV/\AA}$ . The relaxed structure is in good agreement with experimental results. The same structure was then used for some of the AFM states ( $S = 0$ ) and  $S = 2$ , as well as for all of the DFT+U calculations. Due to symmetry restrictions, we only simulated the  $S = 4$ ,  $S = 2$  and AFM ( $S = 0$ ) states. For the DFT+U calculations, a self-consistent Hubbard-U method [19] has been incorporated to determine the U value for Ni, which turns out to be  $6.20 \text{ eV}$  for this system. For oxygen, we took the well-established U value of  $5.90 \text{ eV}$  [23]. For the DOS and projected DOS, we used  $0.1 \text{ eV}$  gaussian smearing to smooth the results.

The DFT calculations confirmed Park et al.'s findings. The optimized structure is shown in Figure 1(a). In order to better display the geometry, we hide all hydrogen atoms. The four nickel atoms and four oxygen atoms on the hmp group (we call them O(1) from now on) define a slightly distorted cube. The AFM state ( $S = 0$ ) turns out to be the ground state, which is  $14.8 \text{ meV}$  lower than the  $S = 2$  state and  $35.1 \text{ meV}$  lower than the  $S = 4$  state (table I, column DFT). Using Löwdin's charge analysis, one can see that about a  $1.48\text{--}1.50 \mu_B$  magnetic moment is found on each nickel atom, and each of the four O(1) atoms contributes a  $0.1\text{--}0.26 \mu_B$  magnetic moment (table II, column DFT). The Heisenberg Hamiltonian in general can be written as:

$$H_{ex} = \sum_{i < j} J_{ij} \mathbf{S}_i \cdot \mathbf{S}_j. \quad (1)$$

Considering the molecule's  $S_4$  symmetry (Figure 1(b)), the six  $J_{ij}$ s reduced to just two values, i.e.:

$$H_{ex} = J_1(\mathbf{S}_1 \cdot \mathbf{S}_2 + \mathbf{S}_2 \cdot \mathbf{S}_3 + \mathbf{S}_3 \cdot \mathbf{S}_4 + \mathbf{S}_4 \cdot \mathbf{S}_1) + J_2(\mathbf{S}_1 \cdot \mathbf{S}_3 + \mathbf{S}_2 \cdot \mathbf{S}_4). \quad (2)$$

We then determined these exchange coupling constants by fitting the expression of Eq. (2) to the obtained energies of the  $S = 4, 2$  and  $0$  spin states, giving  $J_1 = 3.54 \text{ meV}$  and  $J_2 = 2.12 \text{ meV}$ . The positive sign for both numbers indicates AFM coupling. From the total electronic density of states (DOS), as well as the projected density of states (PDOS) onto Ni (Figure 2), it is clear that, in the DFT calculation, the nickel atom 3d orbitals dominate both the highest occupied (HOMO) and lowest unoccupied molecular orbitals (LUMO), so that the HOMO-LUMO gap is of the d-d type.

The DFT+U calculations were performed in two stages. In the first stage (we call this DFT +  $U^d$ ), we turned on the Hubbard-U parameter for the nickel 3d orbitals only, like most current DFT+U calculations; in the second stage (we call this DFT +  $U^{p+d}$ ), we turned on the U parameter for both the nickel 3d and O(1) 2p orbitals. In fact, it is known that Coulomb interactions between oxygen 2p electrons are

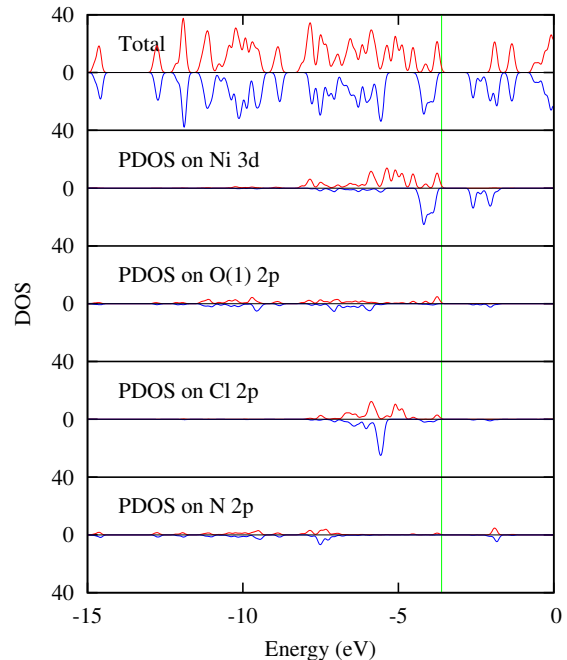


FIG. 2: Total DOS and PDOS on the 2p and 3d orbitals of  $[\text{Ni}(\text{hmp})(\text{MeOH})\text{Cl}]_4$  for the  $S = 4$  state using DFT. Red lines represent  $\alpha$ -spin and blue lines represent  $\beta$ -spin. The green line is the Fermi level,  $E_F$ . The DOS were drawn to the same scale for comparison purposes.

	DFT	DFT + $U^d$	DFT + $U^{p+d}$
AFM ( $S=0$ )	0.0000	0.00000	0.000000
S=2	0.0011	0.00012	-0.000069
S=4	0.0026	0.00019	-0.000368

TABLE I: Total energies in Rydbergs. All numbers are relative to the AFM state ( $S = 0$ )

comparable to those between d electrons [24, 25], and should hence be taken into consideration as well. However, since oxygen usually bears a fully occupied p-shell, this correlation effect is often thought to be negligible. Therefore, in most cases, DFT +  $U^d$  can already yield a satisfactory description of the ground-state without oxygen 2p-electron corrections. Nevertheless, DFT+U has to be taken into consideration explicitly here for both the 3d and oxygen 2p electrons in order to obtain the correct ground state for this molecule.

The DFT+U energies are shown in table I. By turning on DFT+U for the nickel atoms only, the energy differences between different spin states were greatly reduced, hence giving much smaller numbers for the exchange coupling constants. However, the ground state here is still AFM ( $S = 0$ ), and the energies for the  $S = 4$  and  $S = 2$  states relative to the AFM state are  $2.61 \text{ meV}$  and  $1.60 \text{ meV}$ , respectively. But once we take into consideration the strong coulomb interactions for both the Ni and O(1) atoms, the order is reversed, yielding correctly a  $S = 4$  ground state. A spin-

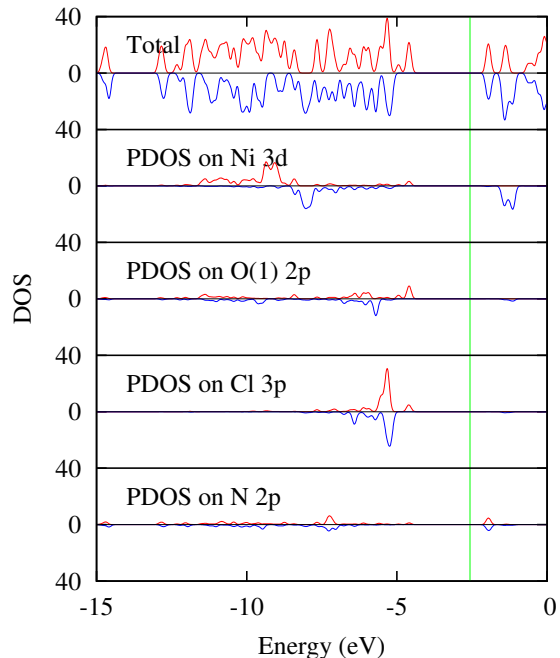


FIG. 3: Total DOS and PDOS on the 2p and 3d orbitals of  $[\text{Ni}(\text{hmp})(\text{MeOH})\text{Cl}]_4$  for the  $S = 4$  state using  $\text{DFT} + U^d$ . Red lines represent  $\alpha$ -spin and blue lines represent  $\beta$ -spin. The green line is the Fermi level,  $E_F$ . DOS were drawn to the same scale for comparison purposes.

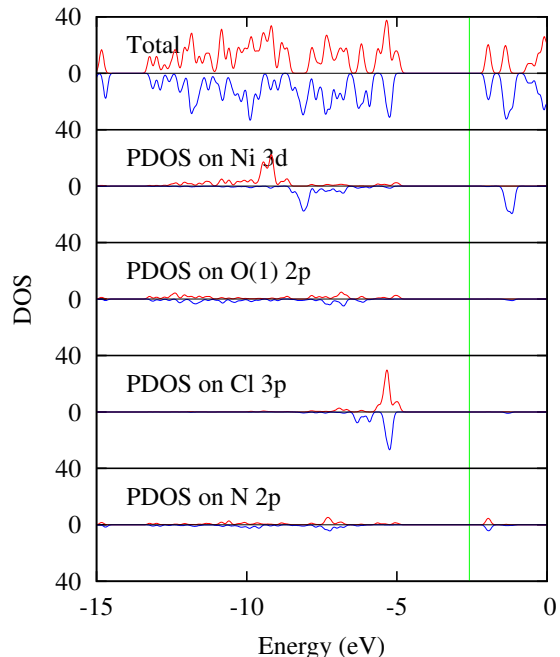


FIG. 4: Total DOS and PDOS on the 2p and 3d orbitals of  $[\text{Ni}(\text{hmp})(\text{MeOH})\text{Cl}]_4$  for the  $S = 4$  ground-state using  $\text{DFT} + U^{p+d}$ . Red lines represent  $\alpha$ -spin and blue lines represent  $\beta$ -spin. The green line is the Fermi level,  $E_F$ . DOS were drawn to the same scale for comparison purposes.

	DFT			DFT + $U^d$			DFT + $U^{p+d}$		
	AFM	S=2	S=4	AFM	S=2	S=4	AFM	S=2	S=4
Ni	1.49	1.49	1.50	1.68	1.68	1.68	1.74	1.74	1.74
O(1)	0.11	0.13	0.26	0.06	0.08	0.16	0.04	0.06	0.11
Cl	0.09	0.09	0.09	0.06	0.06	0.06	0.06	0.06	0.06
N	0.08	0.08	0.08	0.06	0.05	0.05	0.05	0.05	0.05
O(2)	0.06	0.06	0.06	0.03	0.03	0.03	0.03	0.03	0.03

TABLE II: Magnetic moments (in  $\mu_B$ ) captured by Ni, O(1), Cl, N and O(2) atoms. AFM indicates the antiferromagnetic state ( $S = 0$ ). All numbers are averaged over the same species.

unrestricted calculation also confirmed this discovery. The  $S = 2$  state is now 0.94 meV lower than the AFM state, and the  $S = 4$  ground state is 5.00 meV lower. Using these values, we obtained ferromagnetic exchange-coupling constants for the  $\text{DFT} + U^{p+d}$  calculation from a fit to equation 2, i.e.  $J_1 = -0.50$  meV and  $J_2 = -0.68$  meV. These results match experiment reasonably well ( $-0.68$  and  $-2.28$  meV) [26].

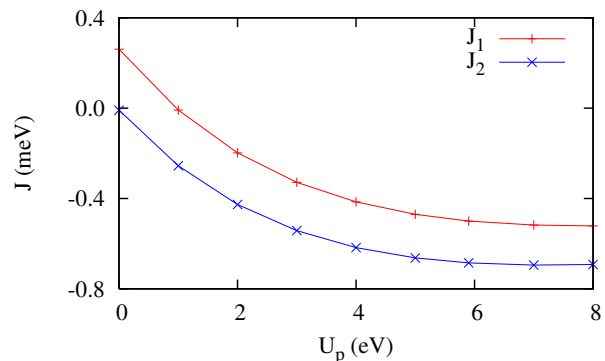


FIG. 5: Variation of  $J_1$  and  $J_2$  with respect to different  $U_p$  for O(1).

To better understand the contribution of the Hubbard- $U$  like term, we first performed Löwdin's charge analysis to calculate the magnetic moments captured by the Ni, O(1), Cl and N and O(2) atoms (table II). The results show that the spin density is more localized in the  $\text{DFT} + U^{p+d}$  calculations ( $1.74 \mu_B$ ) than in normal DFT (around  $1.50 \mu_B$ ), and that the magnetic moments found on the O(1) atoms are greatly reduced. This is because the strong on-site Coulomb interaction prevents the hybridization between the nickel 3d and oxygen 2p orbitals, thus preventing the unphysical "spin-leakage". The DFT calculations favor the AFM ground state because the lack of on-site energy tends to couple electrons with opposite spin projections, and thus lead to the incorrect ground state. The local magnetic moment on an individual atom is a measurable quantity using NMR, and thus can be used to validate these theoretical predictions.

Total DOS and PDOS in the  $\text{DFT} + U^d$  method (Figure 3) and  $\text{DFT} + U^{p+d}$  method (Figure 4) were also calculated [27]. In contrast to the DFT results, the dominant contribution

to the HOMO and LUMO states in both DFT+U calculations is now from the 2p (Cl and O) and 3d (Ni) orbitals, respectively (Figure 4). We do not have direct experimental results to compare with this feature, however, for nickel oxide it is well known that DFT gives incorrect PDOS contributions. Early experiments and calculations [28, 29, 30, 31, 32] show that instead of a d-d gap given by DFT, nickel oxides actually have a p-d gap. The largest spin density contribution, of course, is still from the Ni 3d electrons. For the  $S = 4$  ground state, the DFT +  $U^{p+d}$  calculation yields a LUMO-HOMO gap of 2.95 eV, which is from majority spin to minority spin; in the DFT +  $U^d$  and DFT calculations, these numbers are 2.56 eV and 1.09 eV, respectively. Since DFT has been known to underestimate energy gaps and excitation states, DFT+U calculations have proven necessary in order to obtain agreement with experiments such as resonant inelastic X-ray scattering (RIXS) and XPS [33]. The present study also likely calls into question recent reports of HOMO-LUMO gaps of fractions of an eV in the  $Fe_8$  SMM [34].

Finally, we have also repeated DFT +  $U^d$  and DFT +  $U^{p+d}$  calculations with  $U^d$  for nickel ranging from 4.58 to 6.20 eV and  $U^p$  for oxygen ranging from 1.0 to 8.0 eV. The energetic order of spin states remains the same, and the magnitudes of the energy differences between spin states are more-or-less insensitive to variations of  $U^p$  from 3.0 to 8.0 eV, as seen in Figure 5. This clearly demonstrates the reliability and robustness of our results.

In conclusion, we have performed DFT and DFT+U calculations for  $[Ni(hmp)(MeOH)Cl]_4$ . Because of the strong correlation effects in this system, the DFT calculation fails due to the fact that the lack of on-site energy unphysically encourages the hybridization of orbitals, leading to AFM coupling. The inclusion of a Hubbard-U like term for both the Ni 3d and O(1) 2p electrons greatly enhances the localization for both states, and is essential in order to obtain the correct ferromagnetic ground state and exchange-coupling constants. After taking both corrections into consideration, these properties were successfully reproduced by the calculations. We then analyzed the DOS and projected DOS of the system, and the calculation predicts that the optical transition from HOMO to LUMO is p-d like, and the gap is 2.95 eV.

This work is supported by DOE DE-FG02-02ER45995 (H.-P. Cheng and C. Cao), NSF/DMR/ITR-0218957 (H.-P. Cheng and C. Cao), NSF DMR0239481 (S. Hill), and NSF DMR0506946 (S. Hill). The authors want to thank NERSC, CNMS/ORNL and the University of Florida High Performance Computing Center for providing computational resources and support that have contributed to the research results reported within this paper.

- [2] R. Sessoli, D. Gatteschi, A. Caneschi, et al., *Nature* **365**, 149 (1993).
- [3] R. Sessoli, H.-L. Tsai, A. Schake, et al., *J. Am. Chem. Soc.* **115**, 1804 (1993).
- [4] T. C. Stamatatos, D. Foguet-Albiol, C. C. Stoumpos, et al., *J. Am. Chem. Soc.* **129**, 9484 (2007).
- [5] E.-C. Yang, W. Wernsdorfer, S. Hill, et al., *Polyhedron* **22**, 1727 (2002).
- [6] R. Edwards, S. Maccagnano, E.-C. Yang, S. Hill, et al., *J. Appl. Phys.* **93**, 7807 (2003).
- [7] E. del Barco, A. Kent, E. Yang, et al., *Phys. Rev. Lett.* **93**, 157202 (2004).
- [8] D. N. Hendrickson, E.-C. Yang, R. M. Isidro, et al., *Polyhedron* **24**, 2280 (2005).
- [9] A. Wilson, J. Lawrence, E.-C. Yang, et al., *Phys. Rev. B* **74**, 140403 (2006).
- [10] W. Kohn and L. Sham, *Phys. Rev.* **140**, 1133 (1965).
- [11] M. R. Pederson and S. N. Khanna, *Phys. Rev. B* **60**, 9566 (1999).
- [12] K. Park, M. R. Pederson, and C. S. Hellberg, *Phys. Rev. B* **69**, 014416 (2004).
- [13] K. Park, M. R. Pederson, S. L. Richardson, et al., *Phys. Rev. B* **68**, 020405 (2003).
- [14] T. Baruah and M. Pederson, *Chem. Phys. Lett.* **360**, 144 (2002).
- [15] J. Kortus, M. Pederson, T. Baruah, et al., *Polyhedron* **22**, 1871 (2003).
- [16] D. Venegas-Yazigi, E. Ruiz, J. Cano, and S. Alvarez, *Dalton Trans.* **22**, 2643 (2006).
- [17] K. Park, E.-C. Yang, and D. N. Hendrickson, *J. Appl. Phys.* **97**, 10M522 (2005).
- [18] V. I. Anisimov, J. Zaanen, and O. K. Andersen, *Phys. Rev. B* **44**, 943 (1991).
- [19] M. Cococcioni and S. de Gironcoli, *Phys. Rev. B* **71**, 035105 (2005).
- [20] *PWSCF in Quantum Espresso Package* (2007), URL <http://www.pwscf.org>.
- [21] J. P. Perdew, K. Burke, and M. Ernzerhof, *Phys. Rev. Lett.* **77**, 3865 (1996).
- [22] D. Vanderbilt, *Phys. Rev. B* **41**, 7892 (1990).
- [23] I. Nekrasov, M. Korotin, and V. Anisimov (2007), arXiv:cond-mat/0009107v1.
- [24] M. Norman and A. Freeman, *Phys. Rev. B* **33**, 8896 (1986).
- [25] A. McMahan, R. Martin, and S. Satpathy, *Phys. Rev. B* **38**, 6650 (1988).
- [26] E.-C. Yang, W. Wernsdorfer, L. N. Zakharov, et al., *Inorg. Chem.* **45**, 529 (2006).
- [27] See EPAPS Document No. xxx for enlarged figure showing the PDOS on Cl, O(1) and N atoms. for more information on EPAPS, see <http://www.aip.org/pubservs/epaps.html>.
- [28] J. Zaanen and G. Sawatzky, *J. Solid State Chem.* **88**, 8 (1990).
- [29] P. Wei and Z. Q. Qi, *Phys. Rev. B* **49**, 10864 (1994).
- [30] G. Lee and S.-J. Oh, *Phys. Rev. B* **43**, 14674 (1991).
- [31] A. Shick, A. Liechtenstein, and W. Pickett, *Phys. Rev. B* **60**, 10763 (1999).
- [32] O. Bengone, M. Alouani, P. Blöchl, and J. Hugel, *Phys. Rev. B* **62**, 16392 (2000).
- [33] D. W. Boukhvalov, M. Al-Saqr, E. Z. Kurmaev, et al., *Phys. Rev. B* **75**, 014419 (2007).
- [34] T. Baruah, et al., *Phys. Rev. B* **70**, 214410 (2004).

---

[1] A. Caneschi, D. Gatteschi, R. Sessoli, et al., *J. Am. Chem. Soc.* **113**, 5873 (1991).